tRNA-derived fragments tRF^GlnCTG induced by arterial injury promote vascular smooth muscle cell proliferation

Xiao-Ling Zhu,[1,6] Tao Li,[2,6] Yu Cao,[1,6] Qing-Ping Yao,[3] Xing Liu,[4] Ying Li,[1] Yang-Yang Guan,[1] Ji-Jun Deng,[1] Rui Jiang,[5] and Jun Jiang[1,2]

[1]Department of Thyroid Surgery, The Affiliated Hospital of Southwest Medical University, Luzhou, China; [2]Collaborative Innovation Center for Prevention and Treatment of Cardiovascular Disease of Sichuan Province, Southwest Medical University, Luzhou, China; [3]Institute of Mechanobiology & Medical Engineering, School of Life Sciences & Biotechnology, Shanghai Jiao Tong University, Shanghai, China; [4]Department of Cardiology, The Affiliated Hospital of Southwest Medical University, Luzhou, China; [5]Department of Urology, The Affiliated Hospital of Southwest Medical University, Luzhou, China

tRNA-derived fragments (tRFs) and tRNA halves (tiRNAs) are originated from the specific cleavage of endogenous tRNAs or their precursors and regulate gene expression when the cells are in stressful circumstances. Here, we replicated the rat common carotid artery (CCA) intimal hyperplasia model and investigated the expression of tRFs/tiRNAs in the artery. The normal and the balloon-injured rat CCAs were subjected to small RNA sequencing, and then the differentially expressed tRFs/tiRNAs were identified and analyzed. The expression profiles of tRFs/tiRNAs in the healthy and injured CCAs were remarkably different. tRNA^GlnCTG-derived fragments (tRF^GlnCTG) were found to be overexpressed with a high abundance in the injured CCA. In *in vitro* experiments, the synthetic tRF^GlnCTG mimetics elevated the proliferation and migration of rat vascular smooth muscle cells (VSMCs). Through bioinformatics analysis and an overexpression experiment, tRF^GlnCTG was found to negatively regulate the expression of FAS cell surface death receptor (FAS). This study revealed that tRF^GlnCTG is a crucial regulator in promoting VSMC proliferation. The investigation of the roles of tRFs/tiRNAs is of significance for understanding the mechanism, diagnosis, and treatment of intimal hyperplasia.

INTRODUCTION

Transfer RNAs (tRNAs) are molecules that assemble amino acids into proteins. In recent years, studies have found that when cells are under environmental stress, such as starvation, oxidative stress, or hypoxia, endogenous tRNAs are prone to be cleaved into small fragments at the specific sites.[1] The half molecules formed by the cleavage on the tRNA anticodon loop are called tRNA halves (tiRNAs). The small fragments of tRNA are called tRNA-derived fragments (tRFs). tRFs are approximately 16∼18 nt in length and are derived from mature or precursor tRNA. According to their corresponding position on the parent tRNA, they can be further classified into tRF-5, which corresponds to the 5′ end of mature tRNA and is produced by cleaving the tRNA on the D-loop; tRF-3, which corresponds to the 3′ end of mature tRNA,

is produced by cutting the tRNA on the T-loop, and contains the common carotid artery (CCA) sequence; tRF-1, which is derived from the 3′ tail of the precursor tRNA and includes a poly U sequence at the 3′ end; and i-tRF, which is derived from the internal region of mature tRNA (Figure S1A). Unlike intact tRNAs, tRFs/tiRNAs perform another function: if their nucleic acid sequences are complementary to messenger RNAs (mRNAs), then they interfere with the production of proteins. tRFs/tiRNAs play essential roles in biological regulation and are related to diverse diseases. tiRNA or tRFs are found to be involved in degenerative neural diseases,[2–4] acquired metabolic disorders,[5,6] stress injuries,[7,8] and cancers.[9,10] Their action mechanisms include gene silencing,[11] affecting protein translation,[12] competitive binding to essential proteins,[9,13] and so on.

Intimal hyperplasia is a fundamental pathological change in cardiovascular diseases, such as hypertension and atherosclerosis. It also occurs after vascular surgeries, such as arterial bypass, balloon dilatation and stenting, and arteriovenous fistula. Neointima formation is a crucial cause of vascular stenosis, leading to the failure of revascularization surgery or aggravation of the original disease. There are a variety of cells involved in the formation of neointima. After the endothelium injury, platelets accumulate on the sites where endothelial cells (ECs) fall off, triggering inflammation. Then vascular smooth muscle cells (VSMCs) or adventitial fibroblasts (AFs) accumulate under the intima, hyperproliferating and synthesizing excessive extracellular matrix. In the end, ECs regenerate and cover the intima, reshaping the protective barrier of the intima. In the process of neointima formation, the migration and proliferation of VSMCs play pivotal roles.
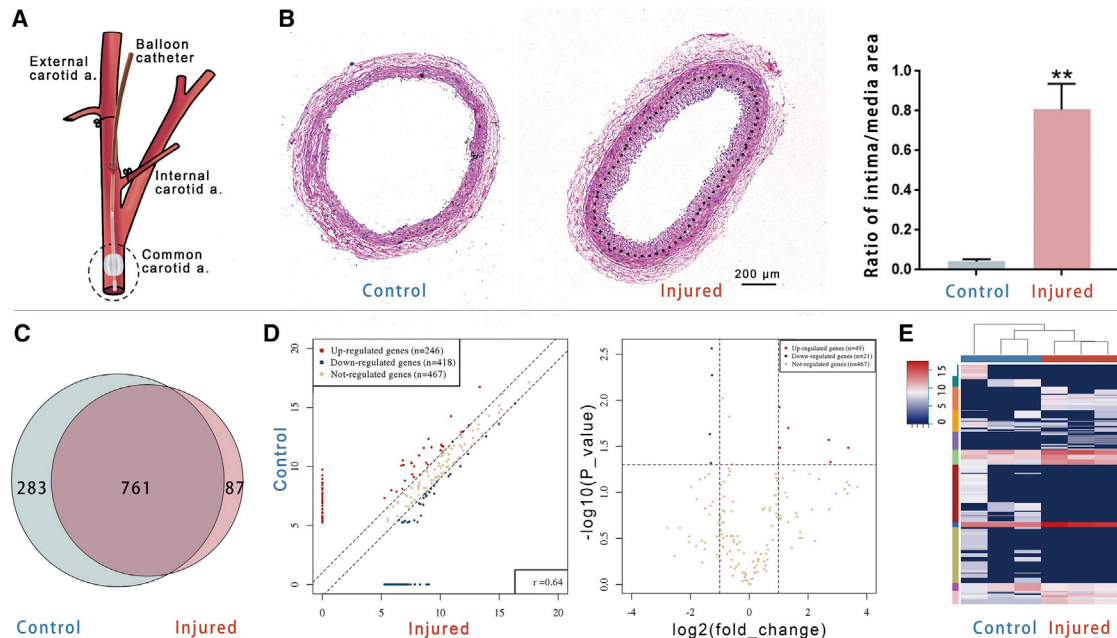
Figure 1. Deep sequencing showed the expression of tRFs and tiRNAs in the rat carotid artery

(A) The schema shows the position of injury to the rat common carotid artery (CCA). (B) Neointima (indicated by a dotted line) appeared in the injured artery 14 days after surgery. The ratio of the intima/media area markedly increased in the injured artery (n = 5). (C) The expression of tRFs and tiRNA in the CCA was detected by deep sequencing. The Venn plot showed the tRF and tiRNA numbers, which were expressed in both of the injured and control CCAs and also indicated the number of specific expression tRFs and tiRNAs. (D) Scatterplot and volcano plot of tRFs and tiRNAs between the healthy and the injured CCAs. tRFs and tiRNAs above the top line (red dots, upregulation) or below the bottom line (blue dots, downregulation) indicate a more than 2.0-fold change between two compared groups. Brown dots show the tRFs and tiRNAs without differential expression. (E) Heatmap of gene expression obtained from the control and the injured CCAs; it includes the 500 tRFs and tiRNAs that have the most significant coefficient of variation (CV) based on tag counts per million of total aligned tRNA reads (TPM). Blue represented an expression level below the mean. Red represented an expression level above the mean (n = 3). Data are expressed as means ± SEM. **p < 0.01.

We hypothesized that as a stress condition, the vascular injury might regulate the production of tiRNA or tRF, which have specific biological effects. In this study, we replicated the rat carotid artery intimal hyperplasia model by balloon injury (Figure 1A) and performed a high-throughput deep RNA sequencing. tiRNA and tRFs were identified and analyzed. One tRF, the tRNA^{GlnCTG}-derived fragment (tRF^{GlnCTG}), was found to be upregulated in the injured arteries. RNA fluorescent *in situ* hybridization (RNA-FISH) demonstrated that tRF^{GlnCTG} was expressed in the cytoplasm of cells from the tunica media and the neointima. The synthesized tRF^{GlnCTG} mimetics promoted VSMC proliferation and migration. In contrast, the inhibitors of tRF^{GlnCTG} suppressed the migration and proliferation of VSMCs. Bioinformatics analysis suggested that tRF^{GlnCTG} may modulate genes involved in cell growth and death. We identified its target genes as FAS cell surface death receptor (FAS). Our study provides new insights for further understanding of intimal hyperplasia mechanism and searching for gene-therapy targets.

RESULTS

The expression profiles of tiRNAs and tRFs were markedly different between the healthy and injured rat CCAs

On day 14 after the balloon injury, the rat CCAs were harvested. Histological sections showed the neointima formed in the carotid artery with a marked increase in the intimal/medial area ratio (Figure 1B). The intimal hyperplasia model was successfully made. Small RNA fragments consistent with pre-tRNA and mature-tRNA sequences were screened from the sequencing results for differential expression analysis between two groups.

The expression profiles of tiRNAs and tRFs in the healthy and injured CCA were markedly different. A total of 1,131 tiRNAs and tRFs were identified, of which 283 were only expressed in normal CCAs, and 87 were exclusively expressed in injured CCAs (Figure 1C). Fragments with expression difference >2.0-fold between the two groups and p values <0.05 were defined as the differentially expressed tiRNAs or tRFs (Figures 1D and 1E). The tiRNAs and tRFs expressed in arteries were mainly tiRNA-5, tRF-5, and i-tRF. Other types, such as tRF-3, tRF-1, and tiRNA-3, just occupied a minimum proportion. The proportion of tRF-5 was higher in the injured arteries than in the healthy arteries (Figure 2A). The source tRNA of tiRNAs and tRFs was also different in the healthy arteries and injured arteries (Figure 2B). There were 14 statistically differentially expressed tiRNAs and tRFs between the healthy and injured arteries (Figure 2C). Nine of them were upregulated, and the other five were downregulated in the injured arteries. In the upregulated tRFs, tRF^{GlnCTG} had a high expression abundance (with high tag
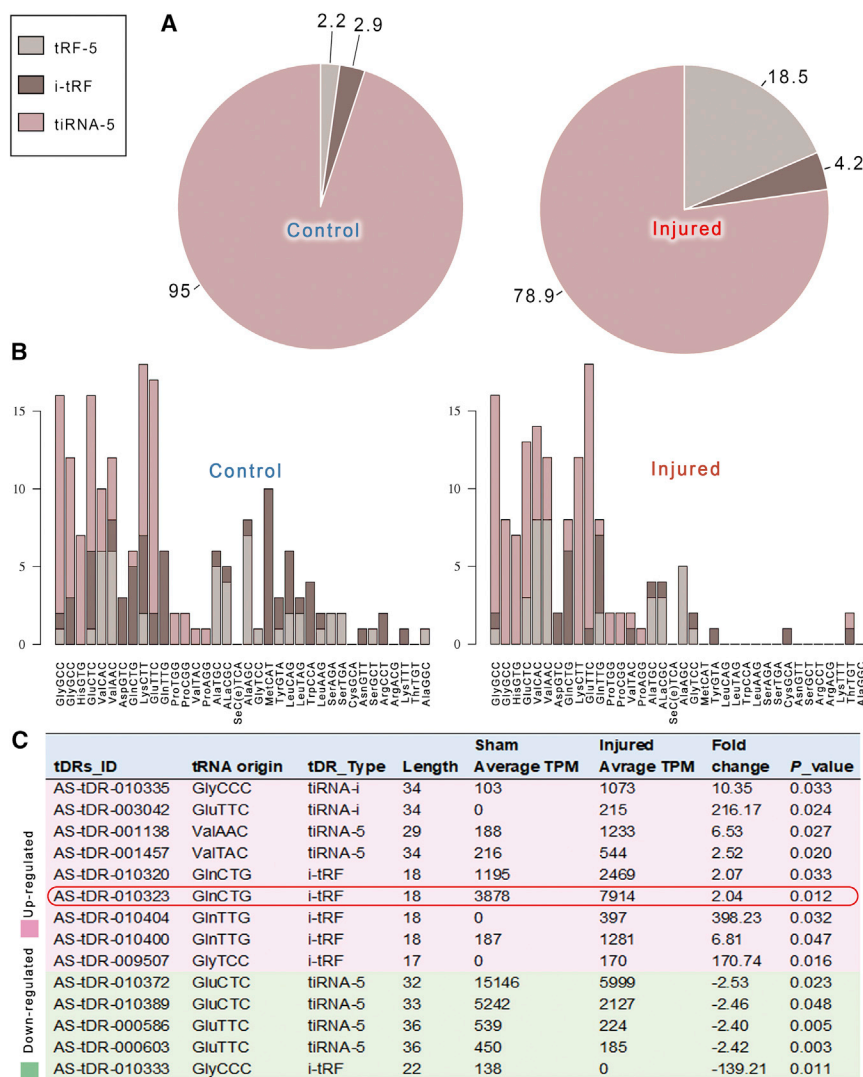
Figure 2. The analysis of the expression of tRFs and tiRNAs in control and injured CCA

(A) Pie plots demonstrated tRF and tiRNA populations in control and injured rat carotid artery. (B) Stacked plots for all subtypes of tRF and tiRNA clustering by the anticodon of the tRNAs. The x axes represent the tRNAs with the same anticodon, and the y axes show the number of all subtype tRFs and tiRNAs derived from the same anticodon tRNA. (C) The gene ID, tRNA origin, type, fold changes, and p value of the differentially expressed tRFs and tiRNAs were given (n = 3). The red box marks tDR-010323 (tRF^{GlnCTG}), which is highly expressed in the rat carotid artery.

	tDRs_ID	tRNA origin	tDR_Type	Length	Sham Average TPM	Injured Avrage TPM	Fold change	*P*_value
Up-regulated	AS-tDR-010335	GlyCCC	tiRNA-i	34	103	1073	10.35	0.033
	AS-tDR-003042	GluTTC	tiRNA-i	34	0	215	216.17	0.024
	AS-tDR-001138	ValAAC	tiRNA-5	29	188	1233	6.53	0.027
	AS-tDR-001457	ValTAC	tiRNA-5	34	216	544	2.52	0.020
	AS-tDR-010320	GlnCTG	i-tRF	18	1195	2469	2.07	0.033
	AS-tDR-010323	GlnCTG	i-tRF	18	3878	7914	2.04	0.012
	AS-tDR-010404	GlnTTG	i-tRF	18	0	397	398.23	0.032
	AS-tDR-010400	GlnTTG	i-tRF	18	187	1281	6.81	0.047
	AS-tDR-009507	GlyTCC	i-tRF	17	0	170	170.74	0.016
Down-regulated	AS-tDR-010372	GluCTC	tiRNA-5	32	15146	5999	-2.53	0.023
	AS-tDR-010389	GluCTC	tiRNA-5	33	5242	2127	-2.46	0.048
	AS-tDR-000586	GluTTC	tiRNA-5	36	539	224	-2.40	0.005
	AS-tDR-000603	GluTTC	tiRNA-5	36	450	185	-2.42	0.003
	AS-tDR-010333	GlyCCC	i-tRF	22	138	0	-139.21	0.011

counts per million of total aligned tRNA reads [TPM] values) in carotid arteries.

tRF^{GlnCTG} was highly expressed in the neointima and also in platelet-derived growth factor (PDGF)-BB- or transforming growth factor (TGF)-β1-induced VSMCs

The results of deep sequencing showed that the expression of tRF^{GlnCTG} was increased in injured arteries (Figure 3A). According to its sequence, tRF^{GlnCTG} was derived from the internal area of tRNA^{GlnCTG} (Figure 3B), so-called i-tRFs. We utilized quantitative real-time PCR to validate its expression in healthy and injured arteries. Its increased expression in injured arteries was confirmed (Figure 3C).

RNA-FISH demonstrated that tRF^{GlnCTG} were localized in the cytoplasm of VSMCs from the tunica media and in the cytoplasm of cells from the neointima. In the neointima, the expression of tRF^{GlnCTG} was markedly elevated (Figure 3D).
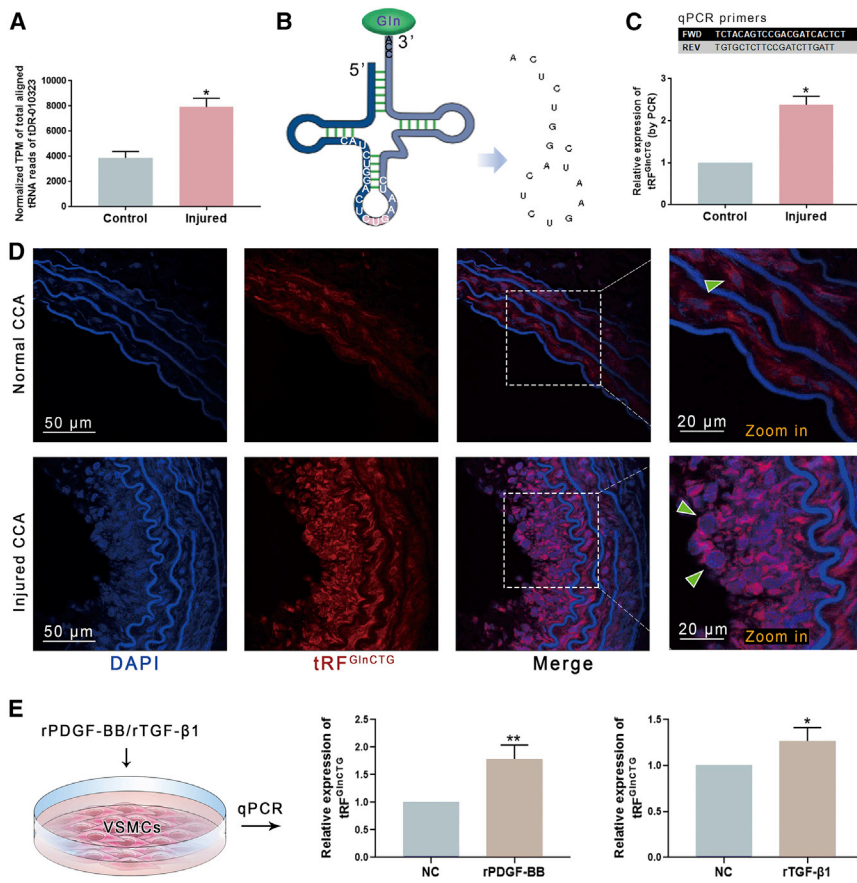
VSMCs from rat thoracic aorta were stimulated with recombinant proteins of PDGF-BB (rPDGF-BB) and TGF-β1 (rTGF-β1) *in vitro*. Both rPDGF-BB and rTGF-β1 resulted in increased expression of tRF^{GlnCTG} (Figure 3E).

tRF^{GlnCTG} promoted the proliferation and viability of VSMCs

We investigated the biological effects of tRF^{GlnCTG} by transfecting the synthetic RNA mimetics or inhibitors into rat VSMCs (Figure 4A).

The Cell Counting Kit-8 (CCK-8) assay showed that the mimetics increased, and the inhibitors decreased the cell viability (Figure 4B).

For the 5-ethynyl-2′-deoxyuridine (EdU) incorporation assay, 50 nM of synthetic tRF^{GlnCTG} mimetics or inhibitors were transfected into VSMCs by Lipofectamine 3000 for 24 h. Then EdU was added to the culture medium. After another 24 h, the number of proliferating cells was counted under a fluorescence microscope, and the cell proliferation rate was calculated. The proliferation of VSMCs transfected with tRF^{GlnCTG} mimetics was increased. On the contrary, tRF^{GlnCTG} inhibitors reduced the number of proliferating cells (Figure 4C).

tRF^{GlnCTG} enhanced the migration of VSMCs

The pretreatment of VSMCs was identical to the cell proliferation assay. Cell motility was assessed by the Transwell and scratch wound-closure assay. The transfection of tRF^{GlnCTG} mimetics significantly increased the migration (Figure 4D) and the wound-closure velocity of VSMCs (Figure 4E). On the other hand, the inhibitors of tRF^{GlnCTG} alleviate cell migration.

Target gene prediction of tRF^{GlnCTG}

In the R environment, TargetScan and miRanda were used to predict the possible target genes of tRF^{GlnCTG}. We performed functional

Figure 3. The expression of tRF^{GlnCTG} in the rat CCAs

(A) Small RNA sequencing demonstrated that tRF^{GlnCTG} was highly expressed in injured CCA (n = 3). (B) tRF^{GlnCTG} is derived from the internal area of mature tRNA^{GlnCTG}. The schema shows its sequence. (C) The real-time qPCR primers were designed according to the sequences of tRF^{GlnCTG} and the adaptors to validate its expression in arteries. PCR confirmed that the expression of tRF^{GlnCTG} was elevated in the injured CCA. (D) RNA *in situ* fluorescence demonstrated that tRF^{GlnCTG} localized in the cytoplasm of VSMCs from tunica media and neointima. It was highly expressed in the neointima (n = 5). (E) Recombinant PDGF-BB and TGF-β1 were used to stimulate cultured VSMCs, and both elevated the expression of tRF^{GlnCTG} (n = 5). Data are expressed as means ± SEM. *p < 0.05, **p < 0.01.

enrichment and pathway prediction of the assumed genes by Gene Ontology (GO) and Kyoto Encyclopedia of Genes and Genomes (KEGG) analysis (Figure 5A). The genes were functionally clustered, and genes related to cell growth, proliferation, death, and movement were paid attention. By querying the results of the GEO (GEO: GSE48279), we found that some of the assumed genes were downregulated in intimal hyperplasia and were previously reported to be involved in vascular biology. These target genes may be involved in the regulation of vascular cell death and movement.

The biological processes and signaling pathways of the potential target genes of TRF^{GlnCTG} were analyzed with Ingenuity Pathway Analysis (IPA) software (QIAGEN Bioinformatics, Hilden, Germany https://www.qiagenbioinformatics.com/products/ingenuitypathway-analysis,content). In the forecasted protein-protein interact networks, ATF6 (activating transcription factor 6), FAS, IL-10 (interleukin 10), MAPK1 (mitogen-activated protein kinase 1), and SPRY2 (Sprouty homolog 2) were located at the hubs of the network (Figure 5B).

FAS was the target gene of tRF^{GlnCTG} in VSMCs

Bioinformatic analysis forecasted the potential binding sites of tRF^{GlnCTG} with AFT6, FAS, IL-10, MAPK1, and SPRY2 (Figure 6A).

These genes have been reported to modulate the growth of vascular cells. The transfection of tRF^{GlnCTG} mimetics to rat VSMCs showed that the level of FAS was decreased, whereas the inhibitors of tRF^{GlnCTG} elevated the level of FAS (Figure 6B). RNAhybrid 2.2 predicted 3 potential binding sites between tRF^{GlnCTG} and FAS mRNA. The binding site with the smallest minimum free energy (MFE) value (−21.4 kcal/mol) (Figure 7A) was consistent with the results predicted by TargetScan and miRanda. We chose this site for the construction of the FAS 3′ UTR luciferase reporter vector. The luciferase reporter assay revealed that tRF^{GlnCTG} mimetics inhibited the expression of FAS mRNA (Figure 7B).

FAS overexpression (FAS-OE) abolished the effect of tRF^{GlnCTG}

To validate the causal link between tRF^{GlnCTG} and FAS, a recombinant lentiviral vector carrying the rat FAS gene was transfected to rat VSMCs, the control group treated with an empty vector. Western blotting confirmed the overexpression of FAS in VSMCs (Figure 7C). Then, the proliferation of FAS-OE VSMCs was investigated under tRF^{GlnCTG} overexpression. FAS-OE VSMCs showed decreased proliferation compared with the control group (Figure 7D). Thus, the results indicated that the overexpression of FAS in VSMCs eliminated the upregulation of proliferation by tRF^{GlnCTG}.

DISCUSSION

Studies have shown that in many species, under certain stressful conditions, such as starvation or hypoxia, endogenous tRNAs or their precursors are prone to be cleaved to produce specific small RNA fragments. Such RNA fragments are a class of gene-expression regulators, and their mechanisms of action are diverse. Some inhibit mRNA translation by microRNAs (miRNAs) manners.[10,14,15] Some serve as reverse transcription primers for the retroviral RNA genome.[16,17] Some are involved in the assembly of precursor rRNA
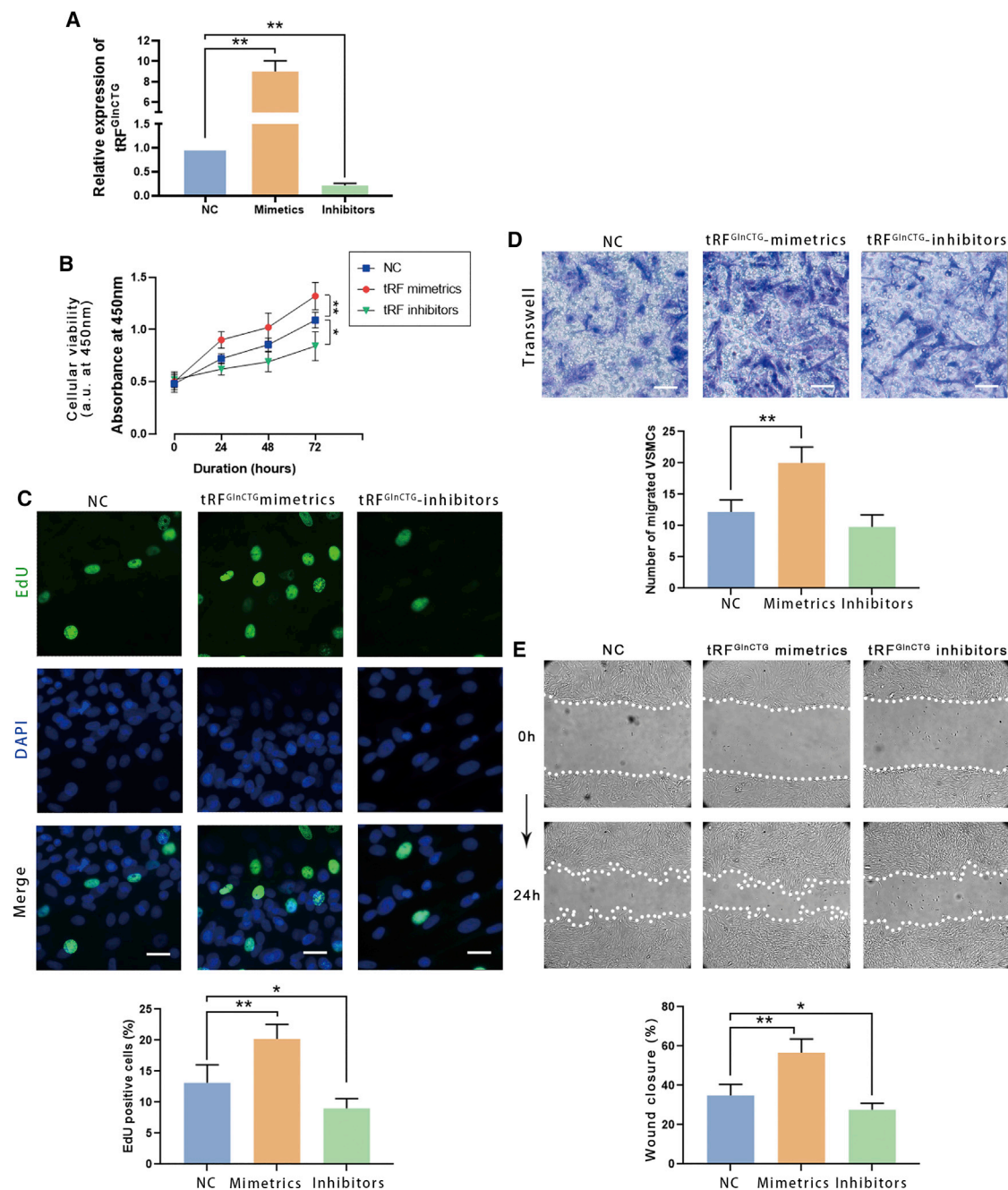
Figure 4. Synthetic tRF^{GlnCTG} mimetics enhanced the proliferation and migration of the cultured rat VSMCs, whereas the inhibitor reduced the proliferation and migration

(A) The transfection efficacy of tRF^{GlnCTG} mimetics and inhibitors was validated by qPCR. (B) Cell counting kit-8 (CCK-8) assay showed that the transfection of tRF^{GlnCTG} mimetics increased DNA synthesis in VSMCs, and the inhibitors reduced it. (C) EdU incorporation assay demonstrated that the tRF^{GlnCTG} mimetics elevated the cell viability, and the inhibitors weakened it. (D) Transwell assay revealed that tRF^{GlnCTG} mimetics induced the migration of VSMCs, and the inhibitors reduced it. (E) Wound-closure assay showed that mimetics accelerated the wound-healing rate, and the inhibitors declined it (n = 5). Data are expressed as means ± SEM. *p < 0.05, **p < 0.01.

cleavage complexes.[18] Others inhibit protein translation.[19] tRFs/ tiRNAs play crucial roles in diseases. For example, CU1276, a tRF from human mature B cells, suppresses proliferation and regulates the molecular response to DNA damage, and it is absent in germinal center-derived lymphomas.[10] tRFs originated from tRNA^{Glu}, tRNA^{Asp}, tRNA^{Gly}, and tRNA^{Tyr} suppress breast cancer metastasis
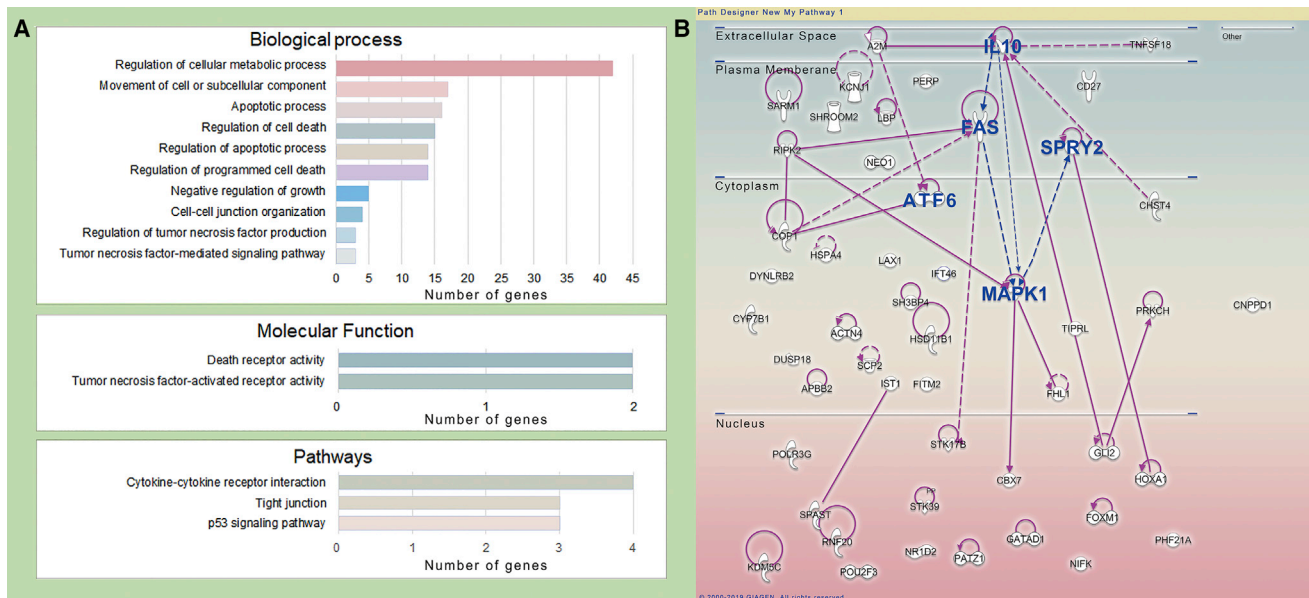
Figure 5. Bioinformatics analysis of tRF^{GlnCTG}

(A) The target genes of tRF^{GlnCTG} were predicted by TargetScan and miRanda. Gene Ontology (GO) and KEGG pathway analysis were performed on these target genes. Here is the number of target genes involved in related biological processes, molecular functions, and pathways. (B) Ingenuity Pathway Analysis (IPA) was used to analyze further the biological processes and signaling pathways of potential target genes. AFT6, FAS, IL-10, MAPK1, and SPRY2 (all highlighted in blue) are located at the predicted protein-protein interaction network hubs.

by competitively binding to YBX1, the stabilizer of pro-oncogenic transcripts.[9]

Vascular injury induces excessive proliferation of the intima, leading to stenosis or even occlusion of blood vessels. We speculate that intimal injury, as a stress condition, may cause changes in tiRNA and tRF expression. The small RNA sequencing to the healthy and injured rat CCA demonstrated that the types and expression levels of tRNA-derived small fragments markedly changed in intimal hyperplasia. A total of 14 differentially expressed tiRNAs and tRFs were identified. Among them, we investigated the regulation of tRF^{GlnCTG} on the biological behavior of VSMCs. Synthetic tRF^{GlnCTG} mimetics promoted the proliferation and migration of VSMCs *in vitro*. On the contrary, inhibitors of tRF^{GlnCTG} weaken VSMC proliferation and migration. Previous studies have also found that tRFs can negatively regulate cell death or apoptosis, promoting cell proliferation.[13,20,21] The change of VSMC biological behavior is pivotal in the process of neointima formation. Therefore, tRF^{GlnCTG} may be essential for the diagnosis and treatment of intimal hyperplasia.

tRNAs are one of the main sources of natural small noncoding RNAs. By bioinformatic tools, we predicted possible target genes of tRF^{GlnCTG}. ATF6,[22–24] FAS,[25–29] IL-10,[30–32] MAPK1,[33,34] and SPRY2[35–38] have been reported to regulate vascular cells' growth. We confirmed that tRF^{GlnCTG} decreased the level of FAS. Furthermore, the overexpression of FAS reduced the proliferation of VSMCs

upregulated by tRF^{GlnCTG}. Studies have shown that the decrease in FAS is one of the critical reasons for intimal hyperplasia. FAS binds to the FAS ligand and forms a death complex, reducing inflammatory cells' infiltration and the proliferation of smooth muscle cells.[26,27] Intimal hyperplasia can be alleviated by local overexpression of the FAS ligand in the arteries injured by the balloon.[25] ECs are relatively resistant to the FAS mechanism. Overexpression of the FAS ligand in transplanted ECs attenuates intimal hyperplasia.[28] The combination of the overexpressing FAS ligand and nitric oxide suppresses smooth muscle growth without affecting endothelium repairment.[29] Our study found that vascular injury induces increased expression of tRF^{GlnCTG}, which promotes neointimal formation by inhibiting FAS (Figure 7E). The tRF^{GlnCTG}-FAS pathway may be one of the mechanisms leading to intimal hyperplasia after arterial injury. The utilization of tRF^{GlnCTG} inhibitors might be a feasible strategy to alleviate neointima formation.

Our understanding of the correlation between tRFs/tiRNAs and vascular biology is still in the preliminary stage. Although we have predicted the possible targets for tRF^{GlnCTG}, the relationship between tRF^{GlnCTG} and neointima formation requires more experiments to determine. Besides, studies of other differentially expressed tRFs and tiRNAs, especially those that are downregulated in intimal hyperplasia, have not been conducted. We hope that shortly, knowledge of the modulation mechanisms of tiRNA and tRFs on vascular biology will be developed and enriched and will provide more tools for the diagnosis and treatment of cardiovascular diseases.
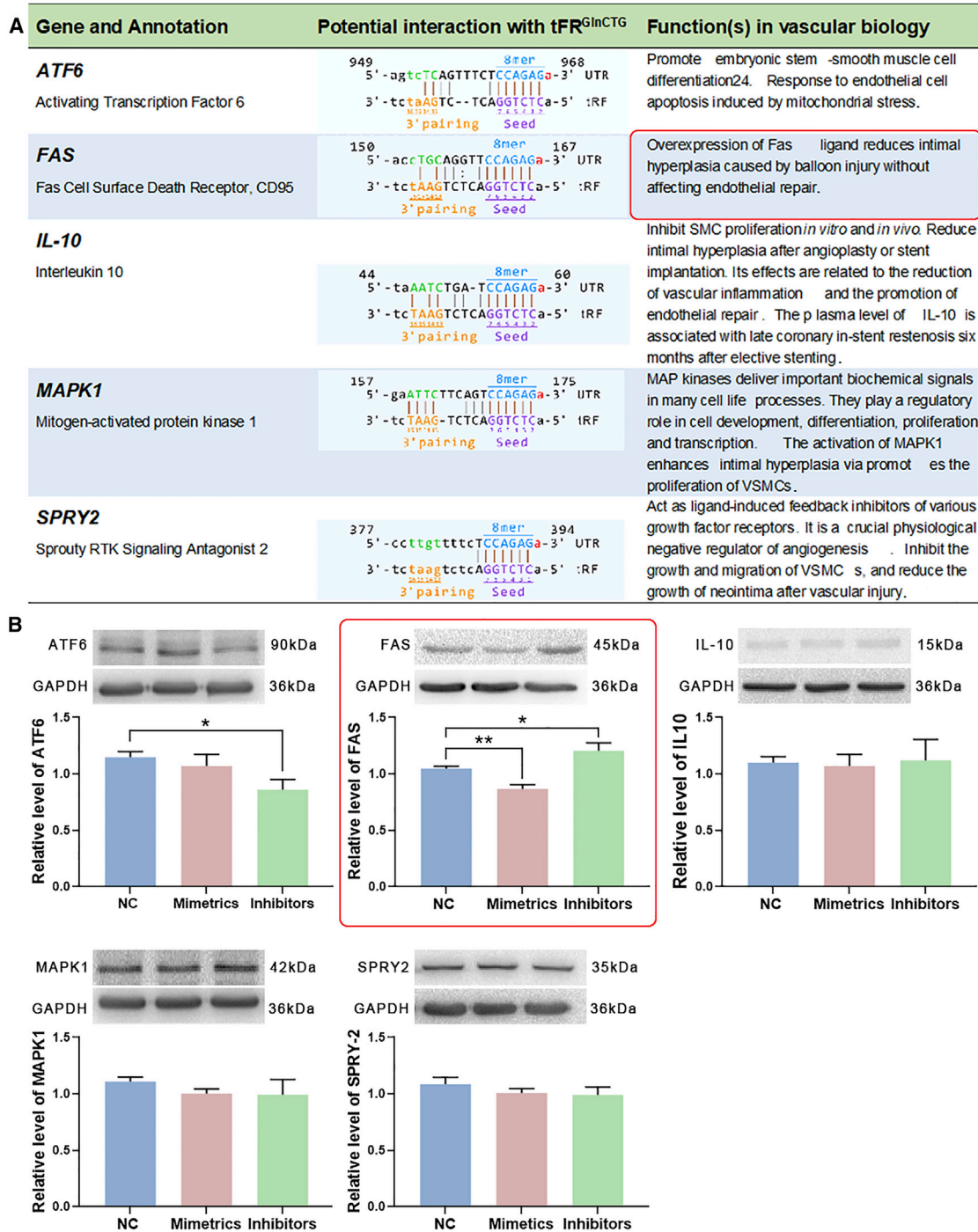
Figure 6. FAS was the target gene of tRF^{GlnCTG} in VSMCs

(A) AFT6, FAS, IL-10, MAPK1, and SPRY2 have been reported to regulate the growth of vascular cells. The possible bindings sites between them and tRF^{GlnCTG} and their functions in vascular biology are listed in the table. (B) Rat VSMCs were transfected with tRF^{GlnCTG} mimetics or inhibitors, and the levels of AFT6, FAS, IL-10, MAPK1, and SPRY2 were detected. tRF^{GlnCTG} mimetics decreased the level of FAS, and the inhibitors increase it (n = 7). Data are expressed as means ± SEM. *p < 0.05, **p < 0.01.
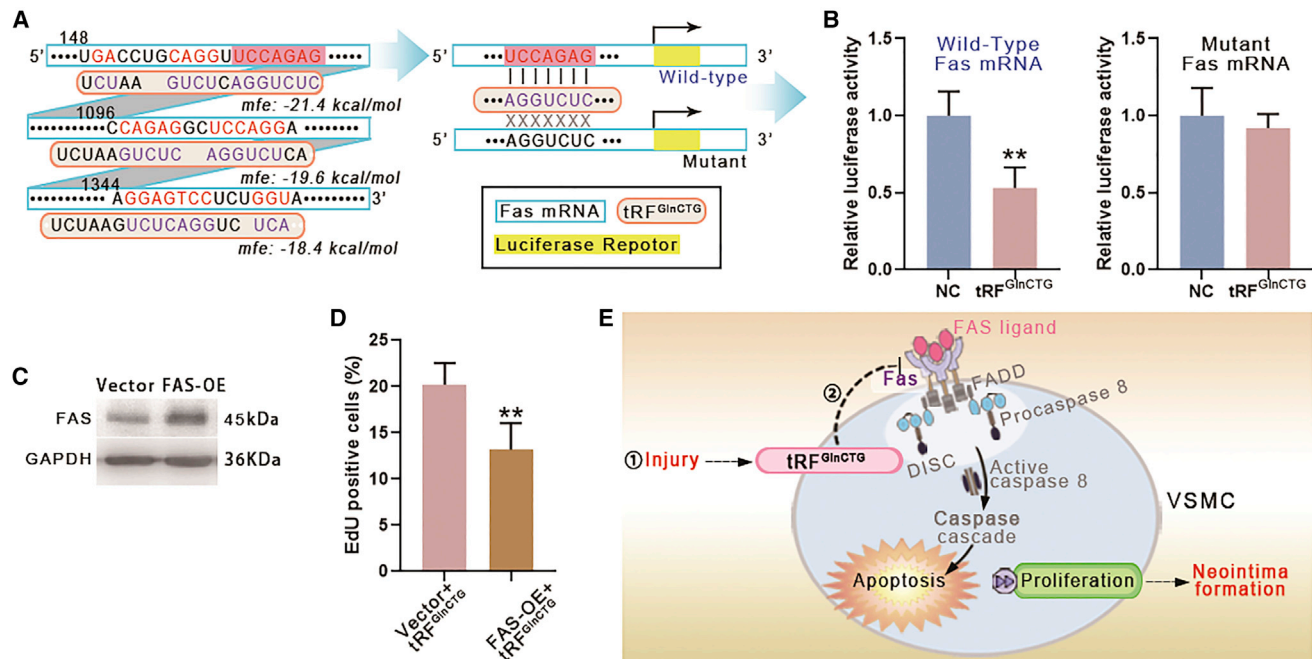
Figure 7. tRF^{GlnCTG} regulated VSMC proliferation via FAS

(A) The potential bindings sites of FAS mRNA and tRF^{GlnCTG} were analyzed by RNAhybrid 2.2. The minimum free energy (MFE) of the binding was labeled on the digraph. The binding site with the smallest MFE value (−21.4 kcal/mol) was consistent with the results predicted by TargetScan and miRanda. We chose this site for the next experiment. (B) Luciferase reporter assay demonstrated that tRF^{GlnCTG} reduced the expression of wild-type FAS mRNA. On the contrary, tRF^{GlnCTG} showed no significant effect on the expression of mutant FAS mRNA. (C) The efficiency of overexpression of FAS in rat VSMC by the lentiviral vector. (D) FAS overexpression reduced the proliferation of VSMCs upregulated by tRF^{GlnCTG} (n = 3). Data are expressed as means ± SEM. **p < 0.01. (E) Schematic diagram of the mechanism of tRF^{GlnCTG} involved in intimal hyperplasia. FAS binds to the FAS ligand and forms a death complex, which activates the caspase cascade and causes cell death. tRF^{GlnCTG} attenuates apoptosis by inhibiting FAS, thereby promoting intimal hyperplasia.

MATERIALS AND METHODS

Intima hyperplasia model of rat CCA

The animal protocol conformed to the Animal Management Rules of China (documentation 55, 2201, Ministry of Health, China) and the recommendations in the 8th edition of the *Guide for the Care and Use of Laboratory Animals* of the NIH (NIH revised 2011). All experiments were approved by the Southwest Medical University Laboratory Animal Care and Use Committee. 8-week-old healthy male Sprague-Dawley rats were anesthetized by intraperitoneal injection of 10% chloral hydrate (300 mg/kg), as described in the previous study.[39] A 2F Fogarty catheter (Edward Lifesciences, Irvine, CA, USA) was inserted into the left CCA of the rat, dragged, and rotated. The right CCA of the rat was dissected, but not invaded, as a sham control. The rats were sacrificed under general anesthesia 14 days after surgery. The bilateral CCAs were harvested, sectioned, and subjected to a small RNA sequencing.

Small RNA sequencing

Total RNA of arteries was extracted by the TRIzol (Thermo Fisher Scientific, Waltham, MA, USA) method. First, the samples were pretreated to remove the modifications, including 3′-aminoacyl, 2′,3′-cyclic phosphate, 5′-OH, m1A, and m3C. With the use of RT primers and amplification primers, cDNA was synthesized and amplified. Sec-

ond, 135−160 bp PCR-amplified fragments (corresponding to a small RNA size of 15∼40 nt) were extracted and purified from the polyacrylamide gel electrophoresis (PAGE) gel. Finally, the completed libraries were quantified by a 2100 Bioanalyzer (Agilent, Santa Clara, CA, USA). The diluted library was sequenced on a NextSeq 500 system (Illumina, San Diego, CA, USA).

The identification and analysis of tiRNA and tRFs

The Illumina chastity filter analyzed the raw sequencing reads data. The sequence of the 5′ and 3′ adaptors was removed from the small RNA data. The trimmed reads conformed to tRNAs were processed to study further. The other small RNAs, including mRNA, rRNA, small nuclear RNA (snRNA), Piwi-interacting RNA (piRNA), small nucleolar RNA (snoRNA), and miRNA, were excluded. Via R software, the differentially expressed tRFs or tiRNAs were hierarchical clustered and made scatterplots.

Quantitative real-time PCR

RNA modifications, including terminal and methylations, were removed using the rtStar tRF&tiRNA Pretreatment Kit (Arraystar, Rockville, MD, USA), according to the manufacturer's instructions. Total RNA of each sample was sequentially ligated to 3′ and 5′ small RNA adaptors, and each adaptor was 60 nt. Therefore, the length of

the amplified cDNA is about 134−160 bp (120 nt + 15−40 nt) (Figure S1B). cDNA was synthesized and amplified using Illumina's proprietary RT primers and amplification primers. With the use of the rtStar First-Strand cDNA Synthesis Kit (Arraystar), cDNA was synthesized and amplified. Stem-loop primers were added into the RT mixtures, and the reaction mixtures were incubated at 95°C for 10 min, followed by 40 cycles of 95°C for 10 s and 60°C for 60 s in a ViiA 7 Real-time PCR System (Applied Biosystems, Foster City, CA, USA). U6 was used as an internal control. The $2^{-\Delta\Delta Ct}$ methods were used for the analysis of the gene expression.

Rat thoracic aorta VSMC culture

As mentioned in the previous study,[40] the rat thoracic aorta was dissected under the aseptic circumstance. First, the tunica adventitia was removed. Subsequently, the ECs on the intima were digested using 0.1% type I collagenase. Finally, the tunica media were cut into small pieces and immersed in DMEM containing 15 mM HEPES, 100 U/mL penicillin, 100 mg/mL streptomycin (Sigma-Aldrich, St. Louis, MO, USA), and 10% newborn bovine serum (Gibco). VSMCs were identified by immunocytochemistry using the anti-alpha-smooth muscle actin (α-SMA) antibody (Cell Signaling Technology, Danvers, MA, USA). Passages 4−7 VSMCs were used for subsequent experiments.

PDGF-BB and TGF-β1 stimulation on VSMCs

VSMCs were cultivated on 6-well plates at a density of 2×10^5 cells with DMEM containing 10% neonatal bovine serum. 25 ng/mL rPDGF-BB (R&D Systems, MN, USA) or 1 ng/mL rTGF-β1 (R&D Systems) was added into the culture medium. The expression of tRF^{GlnCTG} in VSCMs was detected after 24 h by qPCR.

Transfection of RNA mimetics or inhibitors

The exogenous tRF mimetics and inhibitors were synthesized (GenePharma, Shanghai, China.). VSMCs were seeded at a density of 2×10^5 cells/mL and cultured in 6-well plates for 24 h. RNA mimetics or inhibitors were transfected into VSMCs at a final concentration at 50 nM using Lipofectamine 3000 (Thermo Fisher Scientific), according to the manufacturer's protocol.

Cell viability and proliferation assay

VSMCs were transfected with tRF mimetics or inhibitors and then seeded at 5×10^4 cells/mL in a 96-well plate for 48 h. 10 μL of CCK-8 (Dojindo, Kumamoto, Japan) solution was added to the VSMCs, and the cells were incubated at 37 °C. The absorbance was measured at 450 nm using an iMark microplate reader (Bio-Rad, Hercules, CA, USA).

VSMCs were cultured in a 96-well plate for 8 h. 50 μM EdU was added into the culture medium for 2 h. Then the staining solution was added for 30 min in the dark. The proliferation cells were observed using a fluorescence microscope (Olympus BX-51).

Cell migration assay

After transfected with tRF mimetics or inhibitors, VSMCs were seeded at a density of 2×10^5 cells/mL in 24-well plates and cultivated 48 h to the confluence. A 200 μL pipette tip was used to scratch the cell layer to form a wound. The cells were photographed under a BH-2 optical microscope (Olympus, Tokyo, Japan) at 0 h and 24 h after wounding.

A Costar Transwell chamber (pore size of 8 μm; Corning Life Sciences, Tewksbury, MA, USA) containing serum-free DMEM was used to culture VSMCs. The chamber was immersed in the DMEM with 20% fetal bovine serum for 8 h. The unmigrated cells on the inner side of the chamber were removed using a cotton bar. The migrated cells on the chamber's outer side were dyed with crystal violet and counted using an optical microscope.

Bioinformatical analysis

In the R environment, TargetScan and miRanda databases are applied to predict the potential target genes and sites of tRF^{GlnCTG}. The Database for Annotation, Visualization and Integrated Discovery (DAVID) version (v.)6.8 was used to perform the functional clustering of target genes. KEGG pathway was used to analyze the signaling pathways in which target genes may participate. RNAhybrid 2.2 (https://bibiserv.cebitec.uni-bielefeld.de/rnahybrid/submission.html) was used to analyze the potential binding sites and their MFE between tRNA^{GlnCTG} and the target gene.

Western blotting

The rat CCAs or cultured cells' total protein were abstracted using radioimmunoprecipitation assay (RIPA) lysis buffer (Beyotime, Shanghai, China). Proteins were isolated by PAGE and transferred to a nitrocellulose membrane (GE Healthcare Life Sciences, PA, USA). The target proteins were identified with ATF6, FAS, IL-10, MAPK1, and SPRY2 antibodies (Absin, Shanghai, China).

Luciferase reporter assay

1.0×10^4 HEK293T cells were cultured in a 96-well plate. tRF^{GlnCTG} mimetics or nontarget control were diluted in 5 μL of Opti-MEM medium (Beyotime, China). FAS 3′ UTR dual reporter vector (or mutation vector) and 0.25 μL of Lipo6000 transfection reagent (Beyotime, China) were diluted in 5 μL of Opti-MEM medium. The two solutions were mixed gently and added to the cells. The transfection concentration of mimetics was 50 nM. The plasmid concentration was 50 ng/well. After 48 h of transfection, the medium was removed, and luciferase reagent (Promega, Fitchburg, WI, USA) was added. The fluorescence value was measured with a GloMax 96 spectrophotometer (Promega).

Overexpression of FAS

Lentiviral vector overexpressing recombinant FAS (rFAS-OE-LV) encoding FAS (GenBank: NM_139194.2) was obtained by cloning the coding region of FAS from rat VSMC cDNA into lentiviral vector GV492 (GeneChem, Shanghai, China). VSMCs were infected with

FAS-OE-LV particles, and the efficacy of transfection was investigated by western blotting.

Statistical analysis

If there is no specific remark in all of the experiments, then the replicates used in each experimental group are 5 (n = 5). The statistical analysis was processed with Prism 7 (GraphPad, San Diego, CA, USA). Two-tailed Student's t test was performed for pairwise comparison, and a one-way ANOVA was performed for multiple comparisons. Bonferroni corrected p <0.05 was considered statistically significant. The results were expressed as the mean ± standard error of the mean (SEM).

SUPPLEMENTAL INFORMATION

Supplemental Information can be found online at https://doi.org/10.1016/j.omtn.2020.12.010.

ACKNOWLEDGMENTS

AUTHOR CONTRIBUTIONS

J.J. designed the research and wrote and reviewed the manuscript. J.J. and R.J. analyzed the data. X.-L.Z., T.L., Y.C., Q.-P.Y., X.L., Y.L., Y.-Y.G., and J.-J.D. performed the research.

DECLARATION OF INTERESTS

The authors declare no competing interests.

REFERENCES

1. Emara, M.M., Ivanov, P., Hickman, T., Dawra, N., Tisdale, S., Kedersha, N., Hu, G.F., and Anderson, P. (2010). Angiogenin-induced tRNA-derived stress-induced RNAs promote stress-induced stress granule assembly. J. Biol. Chem. 285, 10959–10968.

2. Hanada, T., Weitzer, S., Mair, B., Bernreuther, C., Wainger, B.J., Ichida, J., Hanada, R., Orthofer, M., Cronin, S.J., Komnenovic, V., et al. (2013). CLP1 links tRNA metabolism to progressive motor-neuron loss. Nature 495, 474–480.

3. Greenway, M.J., Andersen, P.M., Russ, C., Ennis, S., Cashman, S., Donaghy, C., Patterson, V., Swingler, R., Kieran, D., Prehn, J., et al. (2006). ANG mutations segregate with familial and 'sporadic' amyotrophic lateral sclerosis. Nat. Genet. 38, 411–413.

4. van Es, M.A., Schelhaas, H.J., van Vught, P.W., Ticozzi, N., Andersen, P.M., Groen, E.J., Schulte, C., Blauw, H.M., Koppers, M., Diekstra, F.P., et al. (2011). Angiogenin variants in Parkinson disease and amyotrophic lateral sclerosis. Ann. Neurol. 70, 964–973.

5. Chen, Q., Yan, M., Cao, Z., Li, X., Zhang, Y., Shi, J., Feng, G.H., Peng, H., Zhang, X., Zhang, Y., et al. (2016). Sperm tsRNAs contribute to intergenerational inheritance of an acquired metabolic disorder. Science 351, 397–400.

6. Sharma, U., Conine, C.C., Shea, J.M., Boskovic, A., Derr, A.G., Bing, X.Y., Belleannee, C., Kucukural, A., Serra, R.W., Sun, F., et al. (2016). Biogenesis and function of tRNA fragments during sperm maturation and fertilization in mammals. Science 351, 391–396.

7. Mishima, E., Inoue, C., Saigusa, D., Inoue, R., Ito, K., Suzuki, Y., Jinno, D., Tsukui, Y., Akamatsu, Y., Araki, M., et al. (2014). Conformational change in transfer RNA is an early indicator of acute cellular damage. J. Am. Soc. Nephrol. 25, 2316–2326.

8. Wang, Q., Lee, I., Ren, J., Ajay, S.S., Lee, Y.S., and Bao, X. (2013). Identification and functional characterization of tRNA-derived RNA fragments (tRFs) in respiratory syncytial virus infection. Mol. Ther. 21, 368–379.

9. Goodarzi, H., Liu, X., Nguyen, H.C., Zhang, S., Fish, L., and Tavazoie, S.F. (2015). Endogenous tRNA-Derived Fragments Suppress Breast Cancer Progression via YBX1 Displacement. Cell 161, 790–802.

10. Maute, R.L., Schneider, C., Sumazin, P., Holmes, A., Califano, A., Basso, K., and Dalla-Favera, R. (2013). tRNA-derived microRNA modulates proliferation and the DNA damage response and is down-regulated in B cell lymphoma. Proc. Natl. Acad. Sci. USA 110, 1404–1409.

11. Venkatesh, T., Suresh, P.S., and Tsutsumi, R. (2016). tRFs: miRNAs in disguise. Gene 579, 133–138.

12. Sobala, A., and Hutvagner, G. (2013). Small RNAs derived from the 5′ end of tRNA can inhibit protein translation in human cells. RNA Biol. 10, 553–563.

13. Saikia, M., Jobava, R., Parisien, M., Putnam, A., Krokowski, D., Gao, X.H., Guan, B.J., Yuan, Y., Jankowsky, E., Feng, Z., et al. (2014). Angiogenin-cleaved tRNA halves interact with cytochrome c, protecting cells from apoptosis during osmotic stress. Mol. Cell. Biol. 34, 2450–2463.

14. Kozomara, A., and Griffiths-Jones, S. (2014). miRBase: annotating high confidence microRNAs using deep sequencing data. Nucleic Acids Res. 42, D68–D73.

15. Schopman, N.C., Heynen, S., Haasnoot, J., and Berkhout, B. (2010). A miRNA-tRNA mix-up: tRNA origin of proposed miRNA. RNA Biol. 7, 573–576.

16. Morris, S., and Leis, J. (1999). Changes in Rous sarcoma virus RNA secondary structure near the primer binding site upon tRNATrp primer annealing. J. Virol. 73, 6307–6318.

17. Ruggero, K., Guffanti, A., Corradin, A., Sharma, V.K., De Bellis, G., Corti, G., Grassi, A., Zanovello, P., Bronte, V., Ciminale, V., and D'Agostino, D.M. (2014). Small non-coding RNAs in cells transformed by human T-cell leukemia virus type 1: a role for a tRNA fragment as a primer for reverse transcriptase. J. Virol. 88, 3612–3622.

18. Couvillion, M.T., Bounova, G., Purdom, E., Speed, T.P., and Collins, K. (2012). A Tetrahymena Piwi bound to mature tRNA 3′ fragments activates the exonuclease Xrn2 for RNA processing in the nucleus. Mol. Cell 48, 509–520.

19. Ivanov, P., Emara, M.M., Villen, J., Gygi, S.P., and Anderson, P. (2011). Angiogenin-induced tRNA fragments inhibit translation initiation. Mol. Cell 43, 613–623.

20. Jiang, X., and Wang, X. (2004). Cytochrome C-mediated apoptosis. Annu. Rev. Biochem. 73, 87–106.

21. Mei, Y., Yong, J., Liu, H., Shi, Y., Meinkoth, J., Dreyfuss, G., and Yang, X. (2010). tRNA binds to cytochrome c and inhibits caspase activation. Mol. Cell 37, 668–678.

22. Wang, X., Karamariti, E., Simpson, R., Wang, W., and Xu, Q. (2015). Dickkopf Homolog 3 Induces Stem Cell Differentiation into Smooth Muscle Lineage via ATF6 Signalling. J. Biol. Chem. 290, 19844–19852.

23. Karamariti, E., Zhai, C., Yu, B., Qiao, L., Wang, Z., Potter, C.M.F., Wong, M.M., Simpson, R.M.L., Zhang, Z., Wang, X., et al. (2018). DKK3 (Dickkopf 3) Alters Atherosclerotic Plaque Phenotype Involving Vascular Progenitor and Fibroblast Differentiation Into Smooth Muscle Cells. Arterioscler. Thromb. Vasc. Biol. 38, 425–437.

24. Karali, E., Bellou, S., Stellas, D., Klinakis, A., Murphy, C., and Fotsis, T. (2014). VEGF Signals through ATF6 and PERK to promote endothelial cell survival and angiogenesis in the absence of ER stress. Mol. Cell 54, 559–572.

25. Luo, Z., Sata, M., Nguyen, T., Kaplan, J.M., Akita, G.Y., and Walsh, K. (1999). Adenovirus-mediated delivery of fas ligand inhibits intimal hyperplasia after balloon injury in immunologically primed animals. Circulation 99, 1776–1779.

26. Mano, T., Luo, Z., Suhara, T., Smith, R.C., Esser, S., and Walsh, K. (2000). Expression of wild-type and noncleavable Fas ligand by tetracycline-regulated adenoviral vectors to limit intimal hyperplasia in vascular lesions. Hum. Gene Ther. 11, 1625–1635.

27. Jiang, C., Yang, Y.F., and Cheng, S.H. (2004). Fas ligand gene therapy for vascular intimal hyperplasia. Curr. Gene Ther. *4*, 33–39.

28. Sata, M., Luo, Z., and Walsh, K. (2001). Fas ligand overexpression on allograft endothelium inhibits inflammatory cell infiltration and transplant-associated intimal hyperplasia. J. Immunol. *166*, 6964–6971.

29. Kural, M.H., Wang, J., Gui, L., Yuan, Y., Li, G., Leiby, K.L., Quijano, E., Tellides, G., Saltzman, W.M., and Niklason, L.E. (2019). Fas ligand and nitric oxide combination to control smooth muscle growth while sparing endothelium. Biomaterials *212*, 28–38.

30. Mazighi, M., Pellé, A., Gonzalez, W., Mtairag, E.M., Philippe, M., Hénin, D., Michel, J.-B., and Feldman, L.J. (2004). IL-10 inhibits vascular smooth muscle cell activation in vitro and in vivo. Am. J. Physiol. Heart Circ. Physiol. *287*, H866–H871.

31. Verma, S.K., Garikipati, V.N., Krishnamurthy, P., Khan, M., Thorne, T., Qin, G., Losordo, D.W., and Kishore, R. (2016). IL-10 Accelerates Re-Endothelialization and Inhibits Post-Injury Intimal Hyperplasia following Carotid Artery Denudation. PLoS ONE *11*, e0147615.

32. Feldman, L.J., Aguirre, L., Ziol, M., Bridou, J.P., Nevo, N., Michel, J.B., and Steg, P.G. (2000). Interleukin-10 inhibits intimal hyperplasia after angioplasty or stent implantation in hypercholesterolemic rabbits. Circulation *101*, 908–916.

33. Pintucci, G., Saunders, P.C., Gulkarov, I., Sharony, R., Kadian-Dodov, D.L., Bohmann, K., Baumann, F.G., Galloway, A.C., and Mignatti, P. (2006). Anti-proliferative and anti-inflammatory effects of topical MAPK inhibition in arterialized vein grafts. FASEB J. *20*, 398–400.

34. Evans, B.C., Hocking, K.M., Osgood, M.J., Voskresensky, I., Dmowska, J., Kilchrist, K.V., Brophy, C.M., and Duvall, C.L. (2015). MK2 inhibitory peptide delivered in nanopolyplexes prevents vascular graft intimal hyperplasia. Sci. Transl. Med. *7*, 291ra95.

35. Taniguchi, K., Sasaki, K., Watari, K., Yasukawa, H., Imaizumi, T., Ayada, T., Okamoto, F., Ishizaki, T., Kato, R., Kohno, R., et al. (2009). Suppression of Sproutys has a therapeutic effect for a mouse model of ischemia by enhancing angiogenesis. PLoS ONE *4*, e5467.

36. Wietecha, M.S., Chen, L., Ranzer, M.J., Anderson, K., Ying, C., Patel, T.B., and DiPietro, L.A. (2011). Sprouty2 downregulates angiogenesis during mouse skin wound healing. Am. J. Physiol. Heart Circ. Physiol. *300*, H459–H467.

37. Biyashev, D., Veliceasa, D., Topczewski, J., Topczewska, J.M., Mizgirev, I., Vinokour, E., Reddi, A.L., Licht, J.D., Revskoy, S.Y., and Volpert, O.V. (2012). miR-27b controls venous specification and tip cell fate. Blood *119*, 2679–2687.

38. Zhang, C., Chaturvedi, D., Jaggar, L., Magnuson, D., Lee, J.M., and Patel, T.B. (2005). Regulation of vascular smooth muscle cell proliferation and migration by human sprouty 2. Arterioscler. Thromb. Vasc. Biol. *25*, 533–538.

39. Xu, J.Y., Chang, N.B., Rong, Z.H., Li, T., Xiao, L., Yao, Q.P., Jiang, R., and Jiang, J. (2019). circDiaph3 regulates rat vascular smooth muscle cell differentiation, proliferation, and migration. FASEB J. *33*, 2659–2668.

40. Xu, J.Y., Chang, N.B., Li, T., Jiang, R., Sun, X.L., He, Y.Z., and Jiang, J. (2017). Endothelial Cells Inhibit the Angiotensin II Induced Phenotypic Modulation of Rat Vascular Adventitial Fibroblasts. J. Cell. Biochem. *118*, 1921–1927.